

## Measurements and Correlation of High-Pressure Densities of Phosphonium Based Ionic Liquids

Luciana I. N. Tomé,<sup>†</sup> Ramesh L. Gardas,<sup>‡</sup> Pedro J. Carvalho,<sup>†</sup> Maria José Pastoriza-Gallego,<sup>§</sup> Manuel M. Piñeiro,<sup>§</sup> and João A. P. Coutinho<sup>\*,†</sup><sup>†</sup>CICECO, Departamento de Química, Universidade de Aveiro, 3810-193 Aveiro, Portugal<sup>‡</sup>Department of Chemistry, Indian Institute of Technology Madras, Chennai 600036, India<sup>§</sup>Departamento de Física Aplicada, Faculdade de Ciências, Universidade de Vigo, E36310 Vigo, Spain Supporting Information

**ABSTRACT:** Experimental density measurements are reported along with the derived thermodynamic properties (isothermal compressibility, isobaric expansivity, and thermal pressure coefficient) for trihexyltetradecylphosphonium-based ionic liquids—chloride, bromide, bis(trifluoromethylsulfonyl)imide, dicyanamide and methyl sulfonate—in the pressure range (0.10 to 45.00 MPa) and temperature range (283.15 to 333.15) K. The effect of the anion of the ionic liquid on the properties under study was evaluated. Experimental densities were correlated using the Tait equation, the modified cell model equation of state, and the Sanchez–Lacombe equation of state, and compared against the predictive method proposed by Gardas and Coutinho. It is shown that the three correlations describe well all the ILs studied, with the Tait equation providing the lowest average relative deviation (less than 0.004 %) and the Sanchez–Lacombe equation of state the highest (inferior to 0.5 %), and that the predicted densities estimated by Gardas and Coutinho method are in good agreement with the experimental densities determined.

## ■ INTRODUCTION

The recognition of remarkable and advantageous properties in ionic liquids (ILs)<sup>1–3</sup> has led, in the past several years, to their widespread application and popularity in numerous and diverse fields.<sup>3–5</sup> A few, among many other possible examples, include their successful use as green alternatives to conventional organic solvents in biotechnology, either in separation and purification processes or in biochemical reactions, in chemical synthesis and catalysis, or in electrochemistry and nanotechnology. ILs have also shown great potential in other applications as, for instance, heat transfer and azeotrope-breaking fluids, stationary phases for chromatography, matrices for mass spectrometry, supports for the immobilization of enzymes or anticorrosion coatings, and electropolishing or antimicrobial agents.<sup>4,6–22</sup>

For the correct design, optimization, and operation of (industrial) processes involving ILs and an efficient exploration of the potentialities of these compounds as designer solvents, the knowledge of their thermophysical properties, such as viscosity, density, and interfacial tension, is required. Although during the past decade the investigation has been intensive and the data bank on the fundamental physical and chemical properties of ILs has increased remarkably,<sup>23–40</sup> the thermophysical characterization of ILs is by no means satisfactory to face the exponential growth of the current scientific and industrial demands. As it is definitely not viable to perform measurements in all ILs due to the high number of combinations of cations and anions possible, there is the need to develop systematic studies on selected systems in order to provide results that can be used to get the basic understanding of their structure–property relationships, to establish adequate correlations and to test predictive methods.

Most of the published work regarding ILs has been focused on imidazolium-based ILs. In spite of the little attention devoted so far to phosphonium-based ILs, their advantageous properties<sup>41–48</sup> have been attracting the industry attention<sup>2</sup> and they are recognized as interesting options for several purposes. Compared to their equivalent imidazolium-based ILs, phosphonium ILs are thermally more stable and less expensive.<sup>41–43</sup> Furthermore, unlike most ILs, they are less dense than water<sup>44,45</sup> and more stable toward nucleophilic and basic conditions because they have no acidic protons.<sup>43</sup> There are also studies showing that these ILs can dissolve larger amounts CO<sub>2</sub> than the corresponding imidazolium ones.<sup>46–48</sup> These characteristics offer greater practicality and scope and have proved to be valuable for many specific applications, for instance, in the purification of biomolecules in aqueous two-phase systems,<sup>12,49</sup> in the separation of ethanol–water mixtures to overcome problems associated to ethanol production,<sup>50</sup> in the extraction of metals<sup>51–53</sup> and of diamondoids from natural gas,<sup>54</sup> and in CO<sub>2</sub> capture and gas separation processes.<sup>46,48,55</sup>

In previous papers we reported experimental data for high pressure densities and derived thermodynamic properties of imidazolium-,<sup>31–34</sup> pyridinium-, pyrrolidinium-, and piperidinium-based ILs<sup>34</sup> and evaluated the influence of the nature of the ionic structures on the properties under study. The results obtained indicated that the density of the ILs can be manipulated by judicious selection of the cation and anion. In a continuation of that systematic study under development, we present, in

Received: November 18, 2010

Accepted: January 20, 2011

Published: March 04, 2011

the current work, experimental measurements of the pressure ( $0.10 < p/\text{MPa} < 45.00$ ) and temperature ( $283.15 < T/\text{K} < 333.15$ ) dependence of the density and derived thermodynamic properties (isothermal compressibility, isobaric expansivity and thermal pressure coefficient) of phosphonium-based ILs and investigate the relationship between the ionic structures and the thermodynamic properties, in order to contribute for the data bank of pure ILs and to establish principles for the molecular design of ILs. For that purpose, the trihexyl(tetradecyl)phosphoniumcation, [THTDP], was studied in combination with five different anions—chloride, [Cl], bromide, [Br], bis(trifluoromethylsulfonyl)imide, [NTf<sub>2</sub>], dicyanamide, [N(CN)<sub>2</sub>], and methyl sulfonate, [CH<sub>3</sub>SO<sub>3</sub>]<sup>−</sup>—to conclude about the anion effect. The experimental densities were correlated using the Tait equation,<sup>56</sup> the Sanchez–Lacombe equation of state (S-L EoS),<sup>57</sup> and the modified cell model equation of state (MCM EoS)<sup>58,59</sup> and compared against the values obtained by the predictive method proposed by Gardas and Coutinho.<sup>60</sup> Derived thermodynamic properties, such as the isothermal compressibility ( $k_T$ ), the isobaric expansivity ( $\alpha_p$ ), and the thermal pressure coefficient ( $\gamma_p$ ), were calculated and reported as Supporting Information. The results obtained for [THTDP][Cl] and [THTDP][NTf<sub>2</sub>] were also compared with previously published data.<sup>28</sup> Thermophysical property data for phosphonium-based ILs are still quite scarce and have seldom been considered.<sup>28,61</sup>

## EXPERIMENTAL SECTION

**Materials.** Experimental densities were measured for five phosphonium-based ILs, namely [THTDP][Cl], [THTDP][Br], [THTDP][NTf<sub>2</sub>], [THTDP][N(CN)<sub>2</sub>], and [THTDP][CH<sub>3</sub>SO<sub>3</sub>]. All of the ILs were kindly provided by Cytec Industries Inc. with mass fraction purities of < 95 %, < 98 %, < 98 %, < 97 %, and < 99 % for the [THTDP][Cl], [THTDP][Br], [THTDP][NTf<sub>2</sub>], [THTDP][N(CN)<sub>2</sub>], and [THTDP][CH<sub>3</sub>SO<sub>3</sub>], respectively.

The ILs were further purified by repeatedly washing them with ultra pure water followed by drying under high vacuum ( $1 \cdot 10^{-3}$  Pa) and moderate temperature (353 K) for a period never inferior to 48 h.<sup>46,62</sup> The water used was double distilled, passed through a reverse osmosis system, and further treated with a Milli-Q plus 18S water purification apparatus. It has a resistivity of 18.2 M $\Omega \cdot \text{cm}$  and a TOC (total organic carbon content) smaller than 5  $\mu\text{g} \cdot \text{dm}^{-3}$ . The purity of each IL was evaluated by <sup>31</sup>P, <sup>1</sup>H, <sup>13</sup>C, and <sup>19</sup>F (only for the [THTDP][NTf<sub>2</sub>]) NMR spectra after each purification step and this procedure was repeated until no impurities were observed in the ILs by NMR analysis. The final purity is estimated to be better than 99 % with a final IL water mass fraction content, determined with a Metrohm 831 Karl Fischer coulometer, of  $33.6 \cdot 10^{-6}$  and (15.95, 28.58, 16.26, and 15.12)  $\cdot 10^{-5}$  for [THTDP][NTf<sub>2</sub>], [THTDP][Br], [THTDP][Cl], [THTDP][CH<sub>3</sub>SO<sub>3</sub>], and [THTDP][N(CN)<sub>2</sub>], respectively. The analyte used for the coulometric Karl Fischer titration was the Hydranal - Coulomat AG from Riedel-de Haën.

## EXPERIMENTAL PROCEDURE

Experimental high pressure densities were determined using an Anton Paar 512P vibrating tube densimeter, connected to an Anton Paar DMA 4500 data acquisition unit. This device determines the vibration period of a metallic U-shape cell filled with the studied fluid, which is directly linked to the sample fluid density. The calibration procedure used in this case has been described previously in detail,<sup>63,64</sup> using water and vacuum as

calibrating references. This method enables the highest accuracy in density determination over wide ranges of pressure, and even reliable density extrapolation, i.e., the determination of density above the reference water values, can be performed. The

**Table 1. Experimental Density ( $\rho$ ) Data for [THTDP][Cl], [THTDP][Br], [THTDP][NTf<sub>2</sub>], [THTDP][N(CN)<sub>2</sub>], and [THTDP][CH<sub>3</sub>SO<sub>3</sub>]**

<i>p</i>	$\rho/(\text{kg} \cdot \text{m}^{-3})$ at <i>T</i> /K					
	283.15	293.15	303.15	313.15	323.15	333.15
	[THTDP][Cl]					
0.10	898.4	892.4	886.5	880.6	874.8	868.9
1.00	898.8	892.9	887.0	881.1	875.3	869.4
2.00	899.3	893.4	887.5	881.7	875.8	870.0
3.00	899.8	893.9	888.0	882.2	876.4	870.6
4.00	900.3	894.4	888.5	882.7	876.9	871.1
5.00	900.7	894.9	889.1	883.3	877.6	871.8
10.0	903.1	897.3	891.5	885.9	880.2	874.5
15.0	905.3	899.6	894.0	888.4	882.8	877.3
20.0	907.5	901.8	896.3	890.8	885.3	879.9
25.0	909.6	904.0	898.6	893.2	887.8	882.5
30.0	911.7	906.3	900.8	895.5	890.1	884.9
35.0	913.7	908.3	903.0	897.7	892.6	887.3
40.0	915.7	910.3	905.1	899.9	894.8	889.6
45.0	917.6	912.4	907.2	902.1	897.0	892.0
	[THTDP][Br]					
0.10	962.7	956.5	950.3	944.1	937.8	931.7
1.00	963.2	957.1	950.9	944.6	938.4	932.3
2.00	963.7	957.6	951.4	945.3	939.0	933.0
3.00	964.2	958.1	952.0	945.8	939.7	933.6
4.00	964.8	958.7	952.6	946.4	940.3	934.2
5.00	965.3	959.2	953.1	947.0	941.0	934.9
10.0	967.9	961.9	955.9	949.8	943.9	938.0
15.0	970.3	964.5	958.6	952.7	946.8	941.0
20.0	972.8	967.0	961.2	955.4	949.7	943.9
25.0	975.3	969.3	963.8	958.0	952.4	946.8
30.0	977.6	971.8	966.3	960.6	955.1	949.6
35.0	979.8	974.2	968.7	963.2	957.7	952.3
40.0	982.0	976.5	971.0	965.5	960.2	954.9
45.0	984.2	978.8	973.4	967.9	962.7	957.3
	[THTDP][NTf <sub>2</sub> ]					
0.10	1077.4	1070.0	1062.7	1055.4	1048.0	1040.8
1.00	1077.9	1070.5	1063.3	1056.0	1048.7	1041.5
2.00	1078.4	1071.2	1063.9	1056.7	1049.3	1042.2
3.00	1079.0	1071.8	1064.5	1057.3	1050.1	1042.9
4.00	1079.6	1072.3	1065.2	1057.9	1050.7	1043.6
5.00	1080.2	1072.9	1065.8	1058.6	1051.4	1044.4
10.0	1083.0	1075.9	1068.8	1061.7	1054.7	1047.8
15.0	1085.6	1078.6	1071.8	1064.9	1057.9	1051.2
20.0	1088.3	1081.4	1074.7	1067.8	1061.0	1054.3
25.0	1090.8	1084.0	1077.4	1070.7	1064.0	1057.4
30.0	1093.3	1086.6	1080.1	1073.5	1066.9	1060.4
35.0	1095.6	1089.1	1082.7	1076.2	1069.8	1063.3
40.0	1097.9	1091.5	1085.1	1078.8	1072.4	1066.2

Table 1. Continued

<i>p</i>	$\rho/(\text{kg}\cdot\text{m}^{-3})$ at <i>T</i> /K					
	283.15	293.15	303.15	313.15	323.15	333.15
45.0	1100.2	1093.9	1087.7	1081.3	1075.1	1068.9
[THTDP][N(CN) <sub>2</sub> ]						
0.10	907.5	901.7	895.9	890.2	884.3	878.6
1.00	908.0	902.1	896.4	890.6	884.8	879.2
2.00	908.4	902.6	896.9	891.2	885.4	879.7
3.00	908.9	903.1	897.4	891.6	885.9	880.2
4.00	909.3	903.5	897.9	892.1	886.5	880.8
5.00	909.8	904.0	898.3	892.7	887.0	881.3
10.0	912.1	906.3	900.7	895.1	889.5	884.0
15.0	914.3	908.5	903.0	897.5	892.0	886.6
20.0	916.2	910.7	905.3	899.9	894.4	889.1
25.0	918.3	912.8	907.5	902.1	896.7	891.4
30.0	920.3	914.9	909.6	904.3	899.0	893.9
35.0	922.2	916.9	911.6	906.5	901.4	896.2
40.0	924.2	918.9	913.7	908.5	903.4	898.3
45.0	926.1	920.9	915.7	910.7	905.6	900.5
[THTDP][CH <sub>3</sub> SO <sub>3</sub> ]						
0.10	938.0	931.8	925.7	919.6	913.4	907.4
1.00	938.4	932.3	926.2	920.1	914.0	908.1
2.00	938.9	932.8	926.7	920.7	914.6	908.7
3.00	939.5	933.4	927.3	921.3	915.3	909.3
4.00	940.1	933.9	927.9	921.9	915.9	910.0
5.00	940.5	934.4	928.4	922.5	916.6	910.6
10.0	943.1	937.1	931.3	925.3	919.5	913.7
15.0	945.6	939.7	934.0	928.1	922.3	916.7
20.0	948.0	942.2	936.6	930.8	925.2	919.6
25.0	950.3	944.6	939.0	933.5	927.9	922.3
30.0	952.7	947.1	941.5	935.9	930.5	925.0
35.0	954.9	949.4	943.8	938.4	933.1	927.7
40.0	957.1	951.6	946.2	940.8	935.5	930.2
45.0	959.3	953.9	948.5	943.3	938.1	932.7

repeatability in the density values determined from the vibration period measured by the DMA 4500 unit is  $10^{-5} \text{ g}\cdot\text{cm}^{-3}$ .

Temperature stability is ensured with a PolyScience 9510 circulating fluid bath, and the temperature value is determined with a CKT100 platinum probe placed in the immediacy of the density measuring cell, with an uncertainty that has been determined to be lower than  $5 \cdot 10^{-2} \text{ K}$ . Pressure is generated and controlled using a Ruska 7610 pressure controller, whose pressure stability is  $2 \cdot 10^{-3} \text{ MPa}$ . The pumping hydraulic fluid (dioctylsebacate fluid) is in direct contact with the fluid sample inside the  $1.59 \cdot 10^{-3} \text{ m}$  diameter steel pressure line conduction, with a coil designed to keep a distance (around 1 m) from the fluid contact interface to the measuring cell, avoiding any diffusion effect.

The combinations of density determination repeatability, and the accuracies in temperature and pressure measurement, lead to an overall experimental density uncertainty value that is lower than  $10^{-4} \text{ g}\cdot\text{cm}^{-3}$  for the whole pressure and temperature range studied in this work.

## RESULTS AND DISCUSSION

Density measurements were carried out at temperatures ranging from (283.15 to 333.15) K and pressures from (0.10 to 45.0)

MPa. The experimental pressure–volume–temperature (PVT) data obtained are reported in Table 1 for all the ILs studied.

Experimental density data for [THTDP][Cl] and [THTDP]-[NTf<sub>2</sub>] are available in literature<sup>28,61</sup> for the pressure and temperature ranges considered in this work. To the best of our knowledge, density results for [THTDP][N(CN)<sub>2</sub>] are only available at atmospheric pressure,<sup>61</sup> and no density data had been previously reported for [THTDP][Br] and [THTDP][CH<sub>3</sub>SO<sub>3</sub>]. The relative deviations between the experimental results obtained in this work and those reported in literature as a function of temperature at 0.10 and 45.0 MPa are presented in Figure 1.

The figure shows that, at atmospheric pressure, experimental density values are in better agreement with Esperança et al.<sup>28</sup> than with Kilaru et al.<sup>61</sup> data, whereas on the other hand, the agreement with the high pressure data of the latter reference is remarkable. This difference in the experimental data trends with Kilaru et al. may be attributed to a calibration issue in their work, taking into consideration the good agreement found with Esperança et al.<sup>28</sup> values for all temperature and pressure ranges studied. The values of [THTDP][Cl] are all lower and an almost constant relative deviation of  $-0.2 \%$  is found for all temperatures and pressures. Nevertheless, slightly higher (more negative) deviations appear at higher pressures. The lowest deviations are observed for [THTDP][NTf<sub>2</sub>], ranging from ( $-0.1 \%$  to  $0.005 \%$ ); for all temperatures considered, the deviations are higher at higher pressure and excellent agreement ( $0.01 \%$ ) is found at low temperature and pressure conditions.

From the experimental densities obtained in this work for the [THTDP]-based ILs, it is observed that the density of the ILs is dependent on the nature of the anion and increases in the order  $\text{Cl} < \text{N}(\text{CN})_2 < \text{CH}_3\text{SO}_3 < \text{Br} < \text{NTf}_2$ . This is the trend observed for the anion dependence of experimental density results for imidazolium-based ILs.<sup>23,65</sup> Moreover, the comparison between the experimental data here reported and available literature data for other classes of ILs (Table 2) shows that, independently of the anion nature, the densities of phosphonium-based ILs are, as expected,<sup>28,61</sup> significantly lower than those of other IL families.

The molar volumes obtained in this work for the series of [THTDP]-based ILs increase with the effective size of the anion and follow the trend  $\text{Cl} < \text{Br} < \text{N}(\text{CN})_2 < \text{CH}_3\text{SO}_3 < \text{NTf}_2$ .

## DENSITY MODELING

**Tait Equation Correlation.** The liquid densities were correlated using the Tait equation,<sup>56</sup> and other thermodynamic properties such as isothermal compressibility,  $k_T$ , the isobaric expansivity,  $\alpha_p$ , and the thermal pressure coefficient,  $\gamma_v$ , were calculated and reported as Supporting Information. The results show that the Tait equation correlates well the data for the pure ILs studied with an average relative deviation (ARD) inferior to  $0.004 \%$ .

The following form of the Tait equation<sup>56</sup>

$$\rho = \frac{\rho(T, P = 0.1 \text{ MPa})}{\left[1 - C \ln \frac{(B + P)}{(B + 0.1)}\right]} \quad (1)$$

where

$$\rho(T, P = 0.1 \text{ MPa}) = a_1 + a_2 T + a_3 T^2 \quad (2)$$

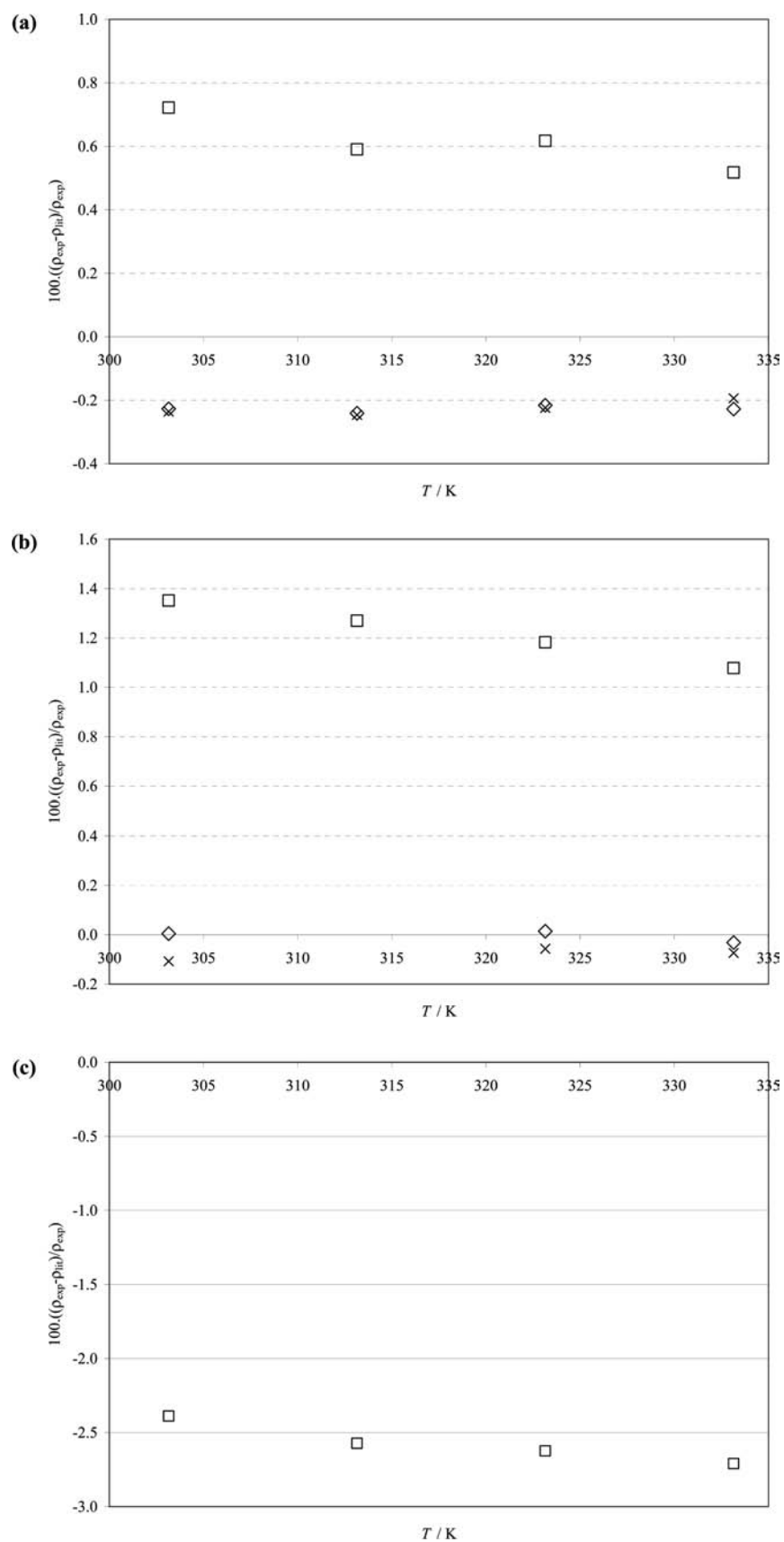


**Figure 1.** Relative deviations between the experimental density data of this work and those reported in literature as a function of temperature, at 0.10 MPa. (a) [THTDP][Cl] at 0.10 MPa:  $\diamond$ , ref 28;  $\square$ , ref 60. [THTDP][Cl] at 45.0 MPa:  $\times$ , ref 60. (b) [THTDP][NTf<sub>2</sub>] at 0.10 MPa:  $\diamond$ , ref 28;  $\square$ , ref 60. [THTDP][NTf<sub>2</sub>] at 45.0 MPa:  $\times$ , ref 60. (c) [THTDP][N(CN)<sub>2</sub>] at 0.10 MPa:  $\square$ , ref 60.

**Table 2.** Experimental Density ( $\rho$ ), Isothermal Compressibility ( $k_T$ ), Isobaric Expansivity ( $\alpha_p$ ), and Thermal Pressure Coefficient ( $\gamma_v$ ) Data of Pure Ionic Liquids Reported in the Literature, at 0.10 MPa<sup>a</sup>

ionic liquid	$\rho$	$k_T$	$\alpha_p \cdot 10^3$	$\gamma_v$	$T$	ref
	kg·m <sup>-3</sup>	GPa <sup>-1</sup>	K <sup>-1</sup>	MPa·K <sup>-1</sup>	K	
[C4mim][Cl]	1080				298.15	65
[C4mim][N(CN) <sub>2</sub> ]	1063.73	0.366	0.6013		293.15	40
[C2mim][NTf <sub>2</sub> ]	1526.0	0.459	0.749	1.632	293.15	32
[C4mim][NTf <sub>2</sub> ]	1441.34	0.514	0.6696	1.208 <sup>b</sup>	293.15	40
[C7mim][NTf <sub>2</sub> ]	1352.8	0.517	0.759	1.468	293.15	32
[C8mim][NTf <sub>2</sub> ]	1328.1	0.515	0.809	1.571	293.15	32
[C10mim][NTf <sub>2</sub> ]	1282.4	0.65	0.7	1.1	293.15	33
[C3mpy][NTf <sub>2</sub> ]	1454.9	0.531	0.723	1.362	293.15	34
[C3mpip][NTf <sub>2</sub> ]	1416.9	0.498	0.719	1.444	293.15	34
[C3mpyr][NTf <sub>2</sub> ]	1438.6	0.507	0.704	1.389	293.15	34
[C4mpyr][NTf <sub>2</sub> ]	1409.1	0.515	0.705	1.368	293.15	34
[N(4)113][NTf <sub>2</sub> ]	1348.3		0.579		298.15	61
[N(4)111][NTf <sub>2</sub> ]	1374.7		0.605		298.15	61
[N(6)222][NTf <sub>2</sub> ]	1279.3		0.579		298.15	61
[N(1)888][NTf <sub>2</sub> ]	1082.3		0.593		298.15	61

<sup>a</sup> [N(4)113], dimethyl(butyl(i-propyl)ammonium; [N(4)111], trimethyl-(butyl)ammonium; [N(6)222], triethyl(hexyl)ammonium; [N(1)888], trioctyl(methyl)ammonium. <sup>b</sup>  $T = 298.15$  K, ref.<sup>27</sup>

was fitted to the density data. In eq 2,  $a_1$ ,  $a_2$ , and  $a_3$  were found by fitting to the experimental  $\rho(T, P = 0.1$  MPa) and are given in Table 3.

Coefficient  $B$  is defined as

$$B = b_1 + b_2 T + b_3 T^2 \quad (3)$$

The coefficients  $C$ ,  $b_1$ ,  $b_2$ , and  $b_3$  were obtained by fitting the Tait equation to experimental data, and their values, along with standard deviation  $\sigma$  of fit are given in Table 4. The standard deviation is defined by

$$\sigma = \left[ \sum_{i=1}^{N_p} (\rho_{\text{calcd}} - \rho_{\text{exptl}})_i^2 / (N_p - k) \right]^{1/2} \quad (4)$$

where  $N_p$  represents the number of data points ( $N_p = 84$ ) and  $k$  is the number of adjusted parameters ( $k = 4$ ). The average relative deviation (ARD) was defined as

$$\text{ARD}(\%) = \frac{\sum_{i=1}^{N_p} |(\rho_{\text{calcd}} - \rho_{\text{exptl}})_i / \rho_{\text{exptl}}|_i}{N_p} \times 100 \quad (5)$$

and is listed in Table 4. A good agreement is found between the experimental density data and isotherms obtained with the Tait equation. A graphical illustration is given in Figure 2 for the case of [THTDP][NTf<sub>2</sub>].

The Tait equation is an integrated form of an empirical equation representative of the isothermal compressibility behavior versus pressure. The effect of pressure in density can be best described by the isothermal compressibility,  $k_T$ , which is

**Table 3.** Coefficients of eq 2, along with Standard Deviation of the Fit ( $\sigma$ )

ionic liquid	$a_1$	$a_2$	$a_3 \cdot 10^7$	$\sigma$
	kg·m <sup>-3</sup>	kg·m <sup>-3</sup> ·K <sup>-1</sup>	kg·m <sup>-3</sup> ·K <sup>-2</sup>	kg·m <sup>-3</sup>
[THTDP][Cl]	1076.483	-0.66212	1.1712	0.03
[THTDP][Br]	1136.618	-0.60838	0.2050	0.03
[THTDP][NTf <sub>2</sub> ]	1296.118	-0.80713	1.2226	0.06
[THTDP][N(CN) <sub>2</sub> ]	1081.095	-0.64255	1.0466	0.05
[THTDP][CH <sub>3</sub> SO <sub>3</sub> ]	1124.578	-0.70102	1.4794	0.04

**Table 4.** Coefficients of eqs 1 and 3, along with Standard Deviation of the Fit ( $\sigma$ ) and Average Relative Deviation (ARD) of eq 1

ionic liquid	$C$	$b_1$	$b_2$	$b_3 \cdot 10^{-4}$	$\sigma$	ARD
			MPa	MPa·K	kg·m <sup>-3</sup>	%
[THTDP][Cl]	0.07646	408.34	-1.2181	9.8188	0.03	0.003
[THTDP][Br]	0.07882	354.22	-0.8128	2.9070	0.05	0.004
[THTDP][NTf <sub>2</sub> ]	0.07965	443.17	-1.4985	14.7738	0.04	0.003
[THTDP][N(CN) <sub>2</sub> ]	0.08057	442.55	-1.3044	10.7345	0.04	0.003
[THTDP][CH <sub>3</sub> SO <sub>3</sub> ]	0.07960	451.63	-1.5470	15.6978	0.04	0.003

calculated according to the following expression:

$$k_T = -\frac{1}{V} \left( \frac{\partial V_m}{\partial P} \right)_T = \frac{1}{\rho} \left( \frac{\partial \rho}{\partial P} \right)_T = \left( \frac{\partial \ln \rho}{\partial P} \right)_T \quad (6)$$

where  $\rho$  is the density and  $P$  the pressure at constant temperature,  $T$ . The isothermal compressibilities can be calculated using eqs 1 and 6

$$k_T = \left( \frac{C}{B + P} \right) \left( \frac{\rho}{\rho(T, P = 0.1 \text{ MPa})} \right) \quad (7)$$

For illustration purposes, the isothermal compressibilities of [THTDP][Cl] are shown in Figure 3. The ILs become more compressible with increasing temperatures and less compressible with increasing pressure. The values obtained for  $k_T$  are given in Table S1 (cf. Supporting Information). In the ranges of temperature (283.15 to 333.15) K and pressure (0.10 to 45.00) MPa considered,  $k_T$  ranges in GPa<sup>-1</sup> are 0.42 to 0.68 for [THTDP][Cl] and [THTDP][Br], and 0.45 to 0.74, 0.40 to 0.63, and 0.44 to 0.72 for, respectively [THTDP][NTf<sub>2</sub>], [THTDP][N(CN)<sub>2</sub>], and [THTDP][CH<sub>3</sub>SO<sub>3</sub>].

The isobaric expansivity,  $\alpha_p$ , is defined as

$$\alpha_p = \frac{1}{V_m} \left( \frac{\partial V_m}{\partial T} \right)_p = -\frac{1}{\rho} \left( \frac{\partial \rho}{\partial T} \right)_p = -\left( \frac{\partial \ln \rho}{\partial T} \right)_p \quad (8)$$

and the following expression is derived from the Tait equation (eq 1)

$$\alpha_p = -\left\{ \frac{[d\rho(T, P = 0.1 \text{ MPa})/dT]}{\rho(T, P = 0.1 \text{ MPa})} \right\} + C \left\{ \frac{\frac{dB}{dT}(P - 0.1)}{\left[ 1 - C \ln \left( \frac{B + P}{B + 0.1} \right) \right] (B + 0.1)(B + P)} \right\} \quad (9)$$

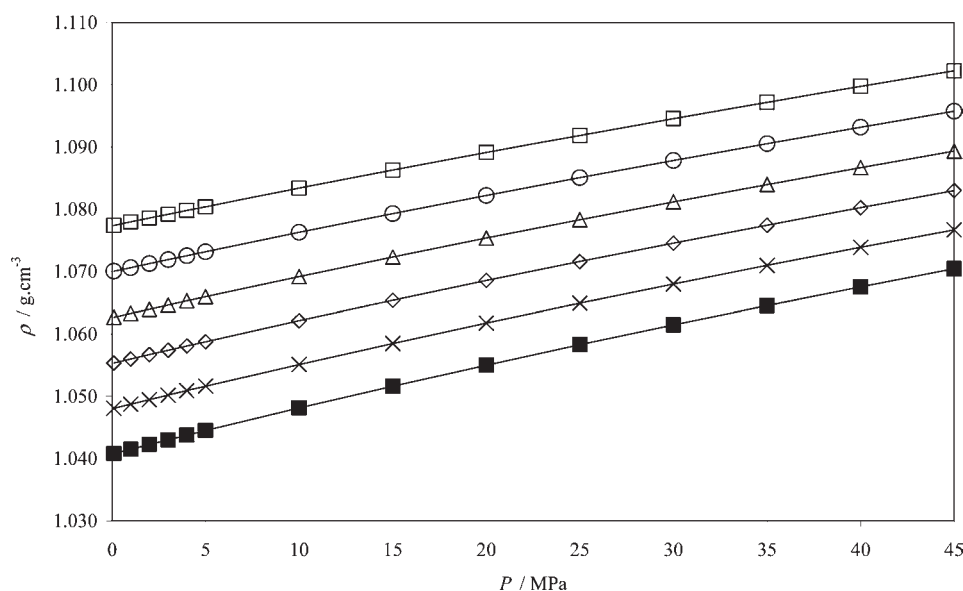


**Figure 2.** Isotherms of the density,  $\rho$ , for [THTDP][NTf<sub>2</sub>]. The symbols refer to the experimental data:  $\square$ , 283.15 K;  $\circ$ , 293.15 K;  $\triangle$ , 303.15 K;  $\times$ , 313.15 K;  $\diamond$ , 323.15 K;  $\blacksquare$ , 333.15 K. The curves were calculated with Tait equation, eq 1.

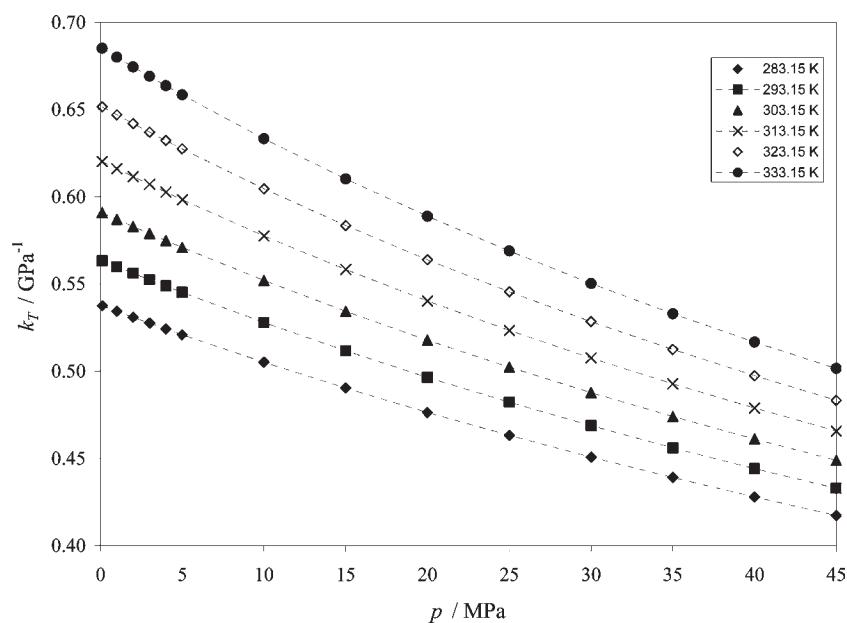


**Figure 3.** Isotherms for the isothermal compressibility,  $k_T$ , of [THTDP][Cl].

where  $d\rho(T, P = 0.1 \text{ MPa})/dT = a_2 + 2a_3T$  and  $dB/dT = b_2 + 2b_3T$ . The data calculated for  $\alpha_p$  of the ILs studied are summarized in Table S2 (cf. the Supporting Information) and the values obtained for [THTDP][NTf<sub>2</sub>] as a function of pressure are depicted in Figure 4. Typically, the value of  $\alpha_p$  of the ILs under study decreases with decreasing temperature for pressures up to 20 MPa. At higher pressures, the increase of temperature originates a decrease in  $\alpha_p$ . In the ranges of temperature (283.15 to 333.15) K and pressure (0.10 to 45.00) MPa, the isobaric expansivity ranges are  $[(0.56 \text{ to } 0.67) \cdot 10^{-3}, (0.55 \text{ to } 0.67) \cdot 10^{-3}, (0.58 \text{ to } 0.70) \cdot 10^{-3}, (0.55 \text{ to } 0.65) \cdot 10^{-3}]$  and  $(0.56 \text{ to } 0.66) \cdot 10^{-3}$  K<sup>-1</sup> for, respectively, [THTDP][Cl], [THTDP][Br], [THTDP][NTf<sub>2</sub>], [THTDP][N(CN)<sub>2</sub>], and [THTDP][CH<sub>3</sub>SO<sub>3</sub>].

The thermal pressure coefficient,  $\gamma_v$ , is calculated according to

$$\gamma_v = \frac{\alpha_p}{k_T} \quad (10)$$

The values of  $\gamma_v$  as a function of pressure for [THTDP][N(CN)<sub>2</sub>] are shown in Figure 5 and the data calculated for the ILs studied are given in Table S3 (cf. the Supporting Information). In general, the values of  $\gamma_v$  decrease with the increase of temperature and with the decrease of pressure. However, the variation of the thermal pressure coefficient of the ILs with pressure is almost non significant for the lowest temperatures considered. By applying the propagation law of errors at eqs 7, 9, and 10 taking into account the uncertainties in the density, temperature, pressure,

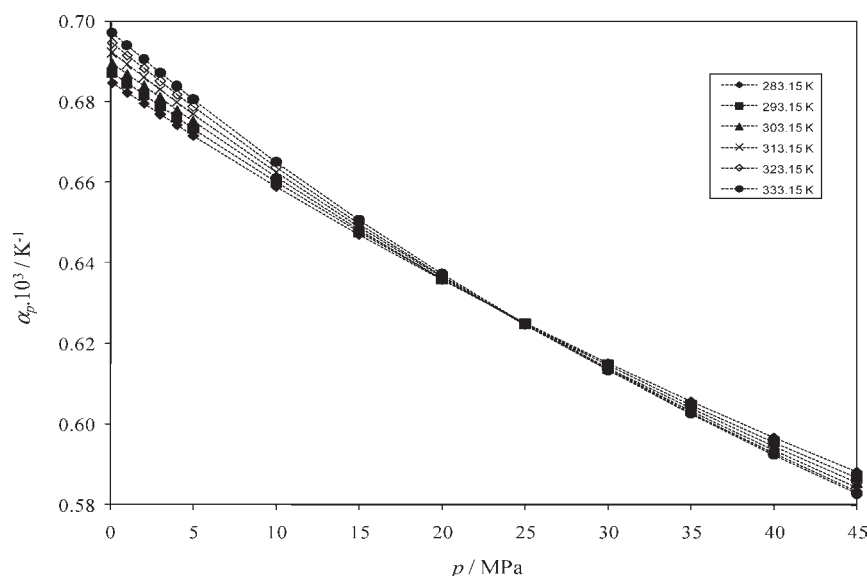


Figure 4. Isotherms for the isobaric expansivity,  $\alpha_p$ , of [THTDP][NTf<sub>2</sub>].

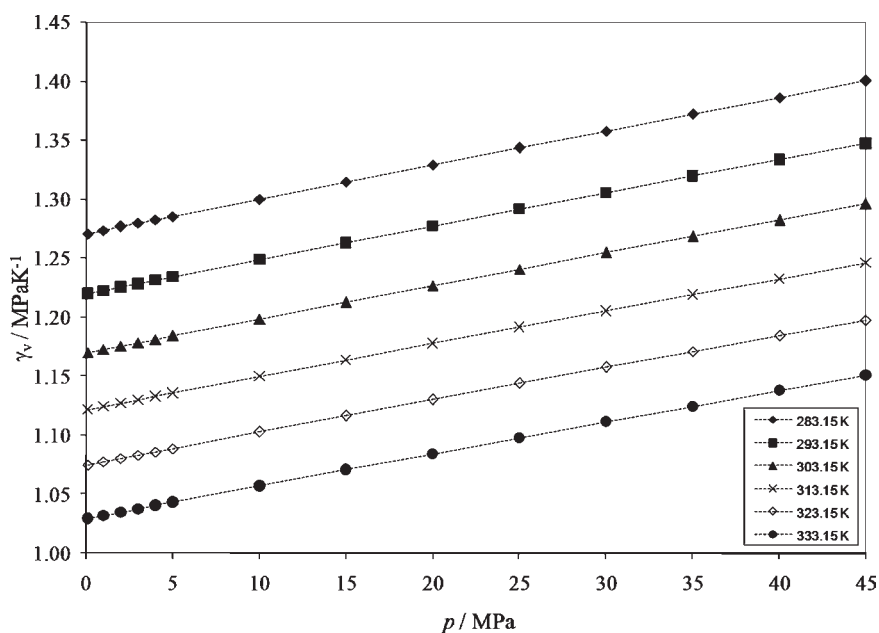


Figure 5. Isotherms for the thermal pressure coefficient,  $\gamma_v$ , of [THTDP][N(CN)<sub>2</sub>].

and coefficients involved in eqs 7, 9, and 10, we obtained an uncertainty of the order of  $\pm 0.05 \text{ GPa}^{-1}$  for  $\kappa_T$ ,  $\pm 5 \cdot 10^{-4} \text{ K}^{-1}$  for  $\alpha_p$ , and  $\pm 1 \text{ MPa} \cdot \text{K}^{-1}$  for  $\gamma_v$ . Uncertainties obtained in  $\gamma_v$  were almost of the same magnitude of the thermal pressure coefficient derived from PVT data.

Unfortunately, as far as authors are aware, there are no data available for comparison of the thermodynamic properties of all the ILs considered in this work since only (rather scarce) results for N(CN)<sub>2</sub>- and NTf<sub>2</sub>- based ILs have been published. From the comparison of the values of  $k_T$  and  $\alpha_p$  available for the N(CN)<sub>2</sub> anion (Table 2) with those of [THTDP][N(CN)<sub>2</sub>], it is observed that these properties are significantly higher when the cation is phosphonium. For [NTf<sub>2</sub>]-imidazolium based ILs, there is an increase of  $k_T$  with the increase of the length of the cation chain (Table 2) and the value of  $k_T$  obtained for [THTDP][NTf<sub>2</sub>] is closer to the

values reported for long chain imidazolium-based ILs. On the other hand, although no clear trend is observed for  $\alpha_p$ , the result obtained for [THTDP][NTf<sub>2</sub>] is similar to those of other IL classes.

**Sanchez–Lacombe Equation of State.** The Sanchez–Lacombe equation of state (S–L EoS) is based on lattice fluid theory<sup>57</sup> and can be used to describe phase equilibria from the pure component parameters. This equation of state is given by the following equations

$$\tilde{\rho}^2 + \tilde{P} + \tilde{T} \left[ \ln(1 - \tilde{\rho}) + \left(1 - \frac{1}{r}\right) \tilde{\rho} \right] = 0$$

$$\tilde{\rho} \equiv \rho/\rho^* \quad \tilde{P} \equiv P/P^* \quad \tilde{T} \equiv T/T^*$$

$$\varepsilon^* = RT^* \quad v^* = RT^*/P^* \quad r = MP^*/RT^*\rho^* \quad (11)$$

**Table 5.** Sanchez–Lacombe Equation of State Parameters, Characteristic Pressure ( $P^*$ ), Temperature ( $T^*$ ) and Density ( $\rho^*$ ), Segment Number of One Molecules ( $r$ ), Segment Interaction Energy ( $\epsilon^*$ ), Segment Volume ( $v^*$ ), and Hard Core Volume ( $v^* \cdot r$ ), and Average Relative Deviation (ARD) of Ionic Liquids

ionic liquid	$P^*$	$T^*$	$\rho^*$	$r$	$\epsilon^*$	$v^*$	$v^* \cdot r$	ARD
	MPa	K	$\text{kg} \cdot \text{m}^{-3}$		$\text{J} \cdot \text{mol}^{-1}$	$\text{cm}^3 \cdot \text{mol}^{-1}$	$\text{cm}^3 \cdot \text{mol}^{-1}$	
[THTDP][Cl]	689.9	497.1	1004.8	86.3	4133	5.99	516.9	0.48
[THTDP][Br]	600.0	507.9	1069.8	74.9	4223	7.04	527.3	0.43
[THTDP][NTf <sub>2</sub> ]	623.0	500.2	1200.5	95.3	4159	6.67	635.7	0.42
[THTDP][N(CN) <sub>2</sub> ]	643.0	509.9	1006.9	82.8	4239	6.59	545.7	0.43
[THTDP][CH <sub>3</sub> SO <sub>3</sub> ]	563.8	561.1	1017.1	68.8	4665	8.27	569.0	0.22

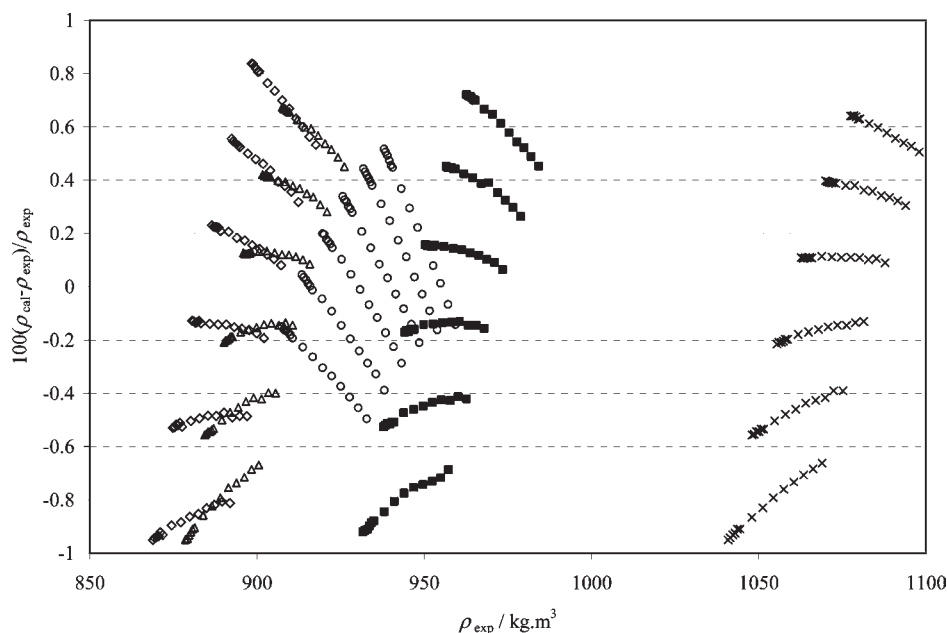


**Figure 6.** Relative deviations between the experimental and calculated density using eq 11 as a function of experimental densities of ILs:  $\diamond$ , [THTDP][Cl];  $\blacksquare$ , [THTDP][Br];  $\times$ , [THTDP][NTf<sub>2</sub>];  $\Delta$ , [THTDP][N(CN)<sub>2</sub>];  $\circ$ , [THTDP][CH<sub>3</sub>SO<sub>3</sub>].

where  $P^*$ ,  $T^*$ , and  $\rho^*$  represent characteristic parameters of the EoS;  $M$  is the molar mass and  $R$  is the gas constant. For the ILs studied, the characteristic parameters were determined by fitting the EoS (eq 11) to the experimental PVT data in the range (283 to 333) K and (0.1 to 45) MPa.

The S–L EoS parameters and the segment number of one molecule ( $r$ ), segment interaction energy ( $\epsilon^*$ ), segment volume ( $v^*$ ), and hard core volume ( $v^* \cdot r$ ) calculated from the S–L EoS parameters are displayed in Table 5. As shown by the ARD values, provided as well in Table 5, the data could be fit to within an ARD of less than 0.5 % for all the ILs. The relative deviations between the experimental and calculated density data as a function of experimental densities, using eq 11, are depicted in Figure 6, for all the ILs considered. The maximum deviation between calculated and experimental density data was within 0.84 % for all the ILs studied.

The free volume ( $V_f$ ) was calculated from

$$V_f = V_m - (v^* \cdot r) \quad (12)$$

where  $V_m$  is the molar volume of the IL at the given  $T$  and  $P$ . This equation has been applied before<sup>33,66</sup> to determine the free volumes of imidazolium-based ILs. Figure 7 shows the free volumes determined from eq 12, as a function of temperature, at 0.1 and

45 MPa. The values of the free volume increase with temperature and decrease with pressure. For the ILs considered in this work,  $V_f$  increases in the order [THTDP][CH<sub>3</sub>SO<sub>3</sub>] < [THTDP][Br] < [THTDP][N(CN)<sub>2</sub>] < [THTDP][Cl] < [THTDP][NTf<sub>2</sub>].

**Modified Cell Model Equation of State.** The MCM EoS has been widely used in the analysis of polymer PVT data<sup>67</sup> and has been recently proved to be able to fit extremely well PVT data of a wide number of ILs, including [THTDP]-based ILs.<sup>68,69</sup> This equation of state is given by

$$\tilde{T} = \frac{\tilde{P}\tilde{V}}{\tilde{V} - 0.8909r - \frac{2}{T} \left( \frac{1.2045^2}{\tilde{V}} - \frac{1.0114}{\tilde{V}} \right)} \quad (13)$$

$$V = \frac{1}{\rho}, \quad \tilde{V} = \frac{V}{V^*}, \quad \tilde{T} = \frac{T}{T^*}, \quad \tilde{P} = \frac{P}{P^*} \quad (14)$$

where  $r$  is constant ( $r = 1.07$ ) and  $P^*$ ,  $T^*$ , and  $V^*$  are characteristic parameters for the given compound and was used to correlate the experimental PVT data in the range (283 to 333) K and (0.1 to 45) MPa. The characteristic parameters, summarized in Table 6, were obtained for each IL studied by minimizing ARD (Table 6) between calculated and experimental density results in the range (283 to 333) K and (0.1 to 45) MPa. The data presented in



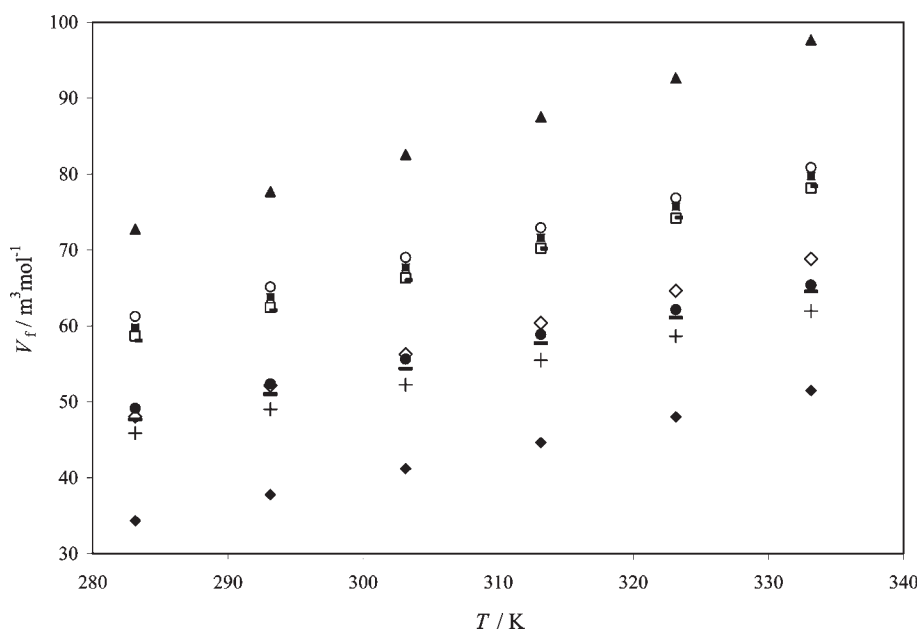


**Figure 7.** Free volume of the ILs studied, [THTDP][Cl]: ○, 0.10 MPa; ●, 45.00 MPa. [THTDP][Br]: □, 0.10 MPa; +, 45.00 MPa. [THTDP][NTf<sub>2</sub>]: ▲, 0.10 MPa; −, 45.00 MPa. [THTDP][N(CN)<sub>2</sub>]: ■, 0.10 MPa; —, 45.00 MPa. [THTDP][CH<sub>3</sub>SO<sub>3</sub>]: ◇, 0.10 MPa; ◆, 45.00 MPa.

**Table 6. Modified Cell Model Equation of State Characteristic Parameters, Pressure ( $P^*$ ), Volume ( $V^*$ ), and Temperature ( $T^*$ ), and Average Relative Deviation (ARD) of Ionic Liquids**

ionic liquid	$P^*$	$V^*$	$T^*$	ARD
	MPa	$\text{cm}^3 \cdot \text{g}^{-1}$	K	%
[THTDP][Cl]	595.4	0.9853	5169	0.01
[THTDP][Br]	567.0	0.9191	5161	0.03
[THTDP][NTf <sub>2</sub> ]	581.0	0.8182	5032	0.06
[THTDP][N(CN) <sub>2</sub> ]	635.1	0.9744	5155	0.04
[THTDP][CH <sub>3</sub> SO <sub>3</sub> ]	562.2	0.9422	5126	0.03

Table 6 shows that the ARD was inferior to 0.06 % for all of the ILs, for 84 data points.

Figure 8 shows the relative deviations between the experimental and calculated density data as a function of experimental densities. The maximum deviation between calculated and experimental density data was within 0.1 % for all the ILs studied

**Gardas and Coutinho Method.** The method proposed by Gardas and Coutinho<sup>59</sup> for the estimation of ionic liquid densities in a wide range of temperatures (273.15 to 393.15) K and pressures (0.10 to 100) MPa is based on eq 15

$$\rho = \frac{M}{NV(a + bT + cP)} \quad (15)$$

here  $\rho$  is the density in  $\text{kg} \cdot \text{m}^{-3}$ ;  $M$  is the molar mass in  $\text{kg} \cdot \text{mol}^{-1}$ ;  $N$  is the Avagadro constant;  $V$  is the molecular volume in  $\text{\AA}^3$ ;  $T$  is the temperature in K, and  $P$  is the pressure in MPa. The coefficients  $a$ ,  $b$ , and  $c$  were estimated by fitting eq 15 to experimental data.<sup>31,32</sup> A total amount of ca. 800 density points were used. The values of coefficients  $a$ ,  $b$ , and  $c$  obtained are, respectively,  $(8.0 \cdot 10^{-1} \pm 2.3 \cdot 10^{-4})$ ,  $(6.7 \cdot 10^{-4} \pm 6.9 \cdot 10^{-7}) \text{ K}^{-1}$  and  $(-5.9 \cdot 10^{-4} \pm 2.4 \cdot 10^{-6}) \text{ MPa}^{-1}$ , at 95 % confidence level. The average relative deviation of calculate densities from

the experimental densities is 0.29 %. The experimental density ( $Y$ ) for the ILs used to obtain coefficients  $a$ ,  $b$ , and  $c$  of eq 15 is essentially identical to its calculated density ( $X$ );  $Y = (0.9998 \pm 0.0003)X$  (correlation coefficient:  $R^2 = 0.9989$ , at 95 % level of confidence). For the density calculation, the molecular volume ( $V$ ) of the [THTDP] cation and of the [NTf<sub>2</sub>] anion were taken from Ye and Shreeve.<sup>68</sup> The molecular volumes of the remaining anions were estimated in this work (Table 7) by minimizing the objective function (O. F.),

$$\text{O.F.} = \frac{\sum_{i=1}^{N_p} |(\rho_{\text{calcd}} - \rho_{\text{exptl}})^2|_i}{N_p} \quad (16)$$

where  $N_p$  represents the number of data points.

The calculated densities using eq 15 and the correspondent ARD of the ILs under study are provided in Table 7 and the relative deviations between the experimental and calculated density data using eq 15 are represented as a function of the experimental densities in Figure 9. As can be seen, the experimental densities ( $Y$ ) of all the ILs considered are in very good agreement with the predicted densities ( $X$ ) from eq 15:  $Y = (1.0095 \pm 0.0068)X$  (correlation coefficient:  $R^2 = 0.9812$ , at 95 % level of confidence). As previously shown in works addressing other families of ionic liquids,<sup>33,34</sup> and reinforced by the results here obtained for phosphonium-based ILs the density estimation method proposed by Gardas and Coutinho<sup>60</sup> can be applied with confidence to ionic liquids from families different than those used on the development of the correlation.

It is worth noting that the molecular volumes provided in this work (Table 7) for Cl, Br, N(CN)<sub>2</sub>, and CH<sub>3</sub>SO<sub>3</sub> anions are rather different from the ones given by Ye and Shreeve,<sup>68</sup> [(47, 56, 88, and 99)  $\text{\AA}^3$ , respectively]. Yet, these new values provide good predictions for Esperança<sup>28</sup> and Kilaru<sup>61</sup> density values of [THTDP][Cl], [THTDP][NTf<sub>2</sub>], and [THTDP][N(CN)<sub>2</sub>] and comparatively good correlations were obtained between

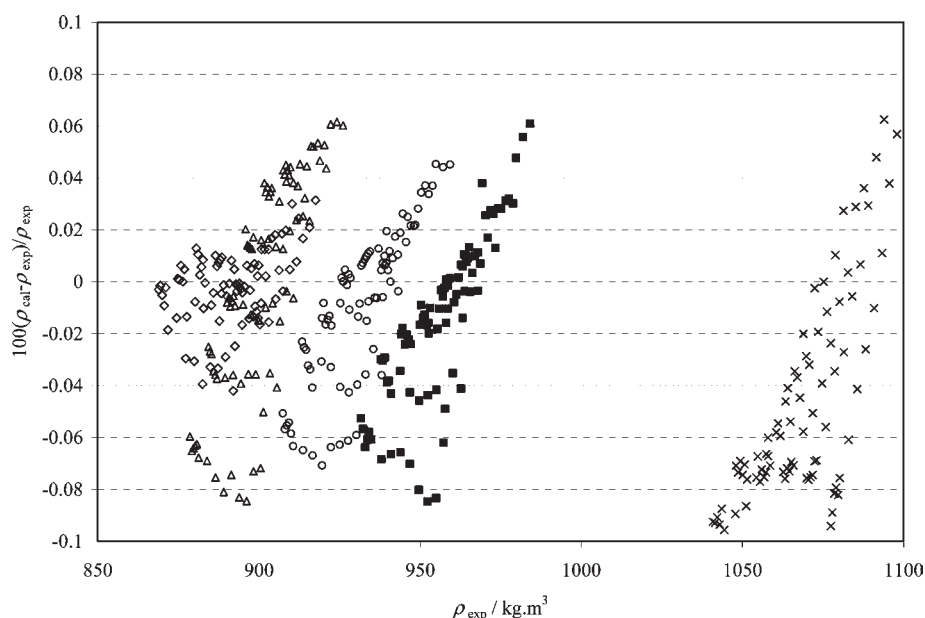


**Figure 8.** Relative deviations between the experimental and calculated density as a function of experimental densities of ILs with the MCM:  $\diamond$ , [THTDP][Cl];  $\blacksquare$ , [THTDP][Br];  $\times$ , [THTDP][NTf<sub>2</sub>];  $\Delta$ , [THTDP][N(CN)<sub>2</sub>];  $\circ$ , [THTDP][CH<sub>3</sub>SO<sub>3</sub>].

**Table 7.** Calculated Densities Using eq 15. Molar Mass ( $M$ ), Molecular Volume ( $V$ ), Experimental Average Density ( $\rho_{\text{expt-av}}$ ), Calculated Average Density ( $\rho_{\text{caled-av}}$ ), and Average Relative Deviation (ARD) of Ionic Liquids

ionic liquid	$M$	$V/\text{\AA}^3$		data points	$\rho_{\text{expt-av}}$	$\rho_{\text{caled-av}}$	ARD
	$\text{g} \cdot \text{mol}^{-1}$	cation	anion		$\text{kg} \cdot \text{m}^{-3}$	$\text{kg} \cdot \text{m}^{-3}$	
[THTDP][Cl]	519.32	947	24	226	891.8	892.3	0.09
[THTDP][Br]	563.76	947	36	84	956.3	956.8	0.09
[THTDP][NTf <sub>2</sub> ]	764.01	947	248	210	1068.9	1066.7	0.24
[THTDP][N(CN) <sub>2</sub> ]	549.90	947	72	84	900.8	900.3	0.17
[THTDP][CH <sub>3</sub> SO <sub>3</sub> ]	578.95	947	89	84	931.7	931.9	0.08

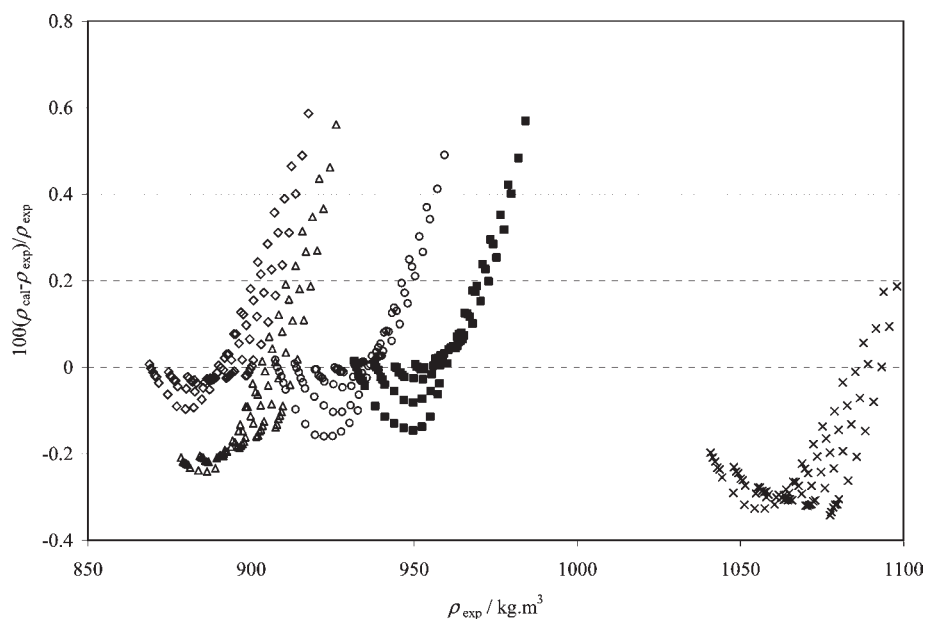


**Figure 9.** Relative deviations between the experimental and calculated density as a function of experimental densities of ILs using eq 15:  $\diamond$ , [THTDP][Cl];  $\blacksquare$ , [THTDP][Br];  $\times$ , [THTDP][NTf<sub>2</sub>];  $\Delta$ , [THTDP][N(CN)<sub>2</sub>];  $\circ$ , [THTDP][CH<sub>3</sub>SO<sub>3</sub>].

the calculated and experimental densities, with relative deviations  $\sim 0.9\%$ .

## CONCLUSIONS

Experimental density data for five phosphonium-based ILs in the temperature range (283.15 to 333.15) K and pressure range (0.10 to 45.0) MPa were provided. From the experimental data, a molar volume increase with the effective anion size is observed.

The experimental results were also used to estimate some derivative thermodynamic properties such as the isothermal compressibility, the isobaric expansivity and the thermal pressure coefficient of the studied ILs that are difficult to obtain by direct measurements at extreme conditions of pressure and temperature.

The liquid densities of the ILs investigated were correlated using the Tait equation, the Sanchez–Lacombe equation of state (S-L EoS) and the modified cell model equation of state (MCM EoS). The results obtained by the three correlations evaluated are very good, with the Tait equation providing the lowest ARD (inferior to 0.004 %). The MCM EoS could correlate the data to within an ARD of 0.06 %. The highest ARD values were obtained with the S-L EoS, but still a good description of the ILs was obtained using this model (less than 0.5 %).

The Gardas and Coutinho method for the prediction of ionic liquid densities was tested against the measured densities and the results show that this predictive method applies to other ionic liquid families than those used for its development.

## ASSOCIATED CONTENT

**S Supporting Information.** Derived thermodynamic properties, such as the isothermal compressibility ( $k_T$ ), the isobaric expansivity ( $\alpha_p$ ), and the thermal pressure coefficient ( $\gamma_v$ ) are calculated and reported. This material is available free of charge via the Internet at <http://pubs.acs.org>.

## AUTHOR INFORMATION

### Corresponding Author

\*Tel: +351-234-370200. Fax: +351-234-370084. E-mail: [jcoutinho@ua.pt](mailto:jcoutinho@ua.pt).

## ACKNOWLEDGMENT

The authors thank financial support from Fundação para a Ciência e a Tecnologia for Project PTDC/EQU FTT/102166/2008 Ph.D. grant (SFRH/BD/41562/2007) of Pedro J. Carvalho and postdoctoral grant SFRH/BPD/44926/2008 of Luciana I. N. Tomé.

## REFERENCES

- (1) Marsh, K. N.; Boxall, J. A.; Lichtenthaler, R. Room temperature ionic liquids and their mixtures - a review. *Fluid Phase Equilib.* **2004**, *219*, 93–98.
- (2) Pletchkova, N. V.; Seddon, K. R. Applications of ionic liquids in the chemical industry. *Chem. Soc. Rev.* **2008**, *37*, 123–150.
- (3) Joglekar, H. G.; Rahman, I.; Kulkarni, B. D. The path ahead for ionic liquids. *Chem. Eng. Technol.* **2007**, *30*, 819–828.
- (4) Zhao, H. Innovative applications of ionic liquids as 'green' engineering liquids. *Chem. Eng. Commun.* **2006**, *193*, 1660–1677.
- (5) Freemantle, M. New frontiers for ionic liquids. *Chem. Eng. News* **2007**, *85*, 23–26.

- (6) Huddleston, J. G.; Willauer, H. D.; Swatoski, R. P.; Visser, A. E.; Rogers, R. D. Room temperature ionic liquids as novel media for clean liquid-liquid extraction. *Chem. Commun.* **1998**, 1765, 1765–1766.

- (7) Poole, C. F.; Poole, S. K. Extraction of organic compounds with room temperature ionic liquids. *J. Chromatogr. A* **2010**, *1217*, 2268–2286.

- (8) Zhao, H.; Xia, S.; Ma, P. Use of ionic liquids as 'green' solvents for extractions. *J. Chem. Technol. Biotechnol.* **2005**, *80*, 1089–1096.

- (9) Wang, J.; Pei, Y.; Zhao, Y.; Hu, Z. Recovery of amino acids by imidazolium-based ionic liquids from aqueous media. *Green Chem.* **2005**, *7*, 196–202.

- (10) Tomé, L. I. N.; Catambas, V. R.; Teles, A. R. R.; Freire, M. G.; Marrucho, I. M.; Coutinho, J. A. P. Tryptophan extraction using hydrophobic ionic liquids. *Sep. Purif. Technol.* **2010**, *72*, 167–173.

- (11) Domínguez-Pérez, M.; Tomé, L. I. N.; Freire, M. G.; Marrucho, I. M.; Cabeza, O.; Coutinho, J. A. P. (Extraction of biomolecules using) aqueous biphasic systems formed by ionic liquids and amino acids. *Sep. Purif. Technol.* **2010**, *72*, 85–91.

- (12) Louros, C. L. S.; Cláudio, A. F. M.; Neves, C. M. S. S.; Freire, M. G.; Marrucho, I. M.; Pauly, J.; Coutinho, J. A. P. Extraction of biomolecules using phosphonium-based ionic liquids+K3PO4 aqueous biphasic systems. *Int. J. Mol. Sci.* **2010**, *11*, 1777–1791.

- (13) Jain, N.; Kumar, A.; Chauhan, S.; Chauhan, S. M. S. Chemical and biochemical transformations in ionic liquids. *Tetrahedron* **2005**, *61*, 1015–1060.

- (14) Welton, T. Room temperature ionic liquids. Solvents for synthesis and catalysis. *Chem. Rev.* **1999**, *99*, 2071–2083.

- (15) Kragel, U.; Eckstein, M.; Kaftzik, N. Enzyme catalysis in ionic liquids. *Curr. Opin. Biotechnol.* **2002**, *13*, 565–571.

- (16) Zhao, H.; Luo, R. G.; Malhotra, S. V. Kinetic study on the enzymatic resolution of homophenylalanine ester using ionic liquids. *Biotechnol. Prog.* **2003**, *19*, 1016–1018.

- (17) Vaher, M.; Borissova, M.; Koel, M.; Kaljurand, M. Ionic liquids as background electrolyte additives and coating materials in capillary electrophoresis. *Proc. Estonian Acad. Sci. Chem.* **2007**, *56*, 187–198.

- (18) Zhao, H.; Malhotra, S. V. Applications of ionic liquids in organic synthesis. *Aldrichim. Acta* **2002**, *35*, 75–83.

- (19) Branco, L. C.; Crespo, J. G.; Afonso, C. A. M. Studies on the selective transport of organic compounds by using ionic liquids as novel supported liquid membranes. *Chem. – Eur. J.* **2002**, *8*, 3865–3871.

- (20) Scovazzo, P.; Kieft, J.; Finan, D. A.; Koval, C.; DuBois, D.; Noble, R. Gas separations using non-hexafluorophosphate [PF6]<sup>-</sup> anion supported ionic liquid membranes. *J. Membr. Sci.* **2004**, *238*, 57–63.

- (21) Buzzeo, M. C.; Evans, R. G.; Compton, R. G. Non-haloaluminate room temperature ionic liquids in electrochemistry - a review. *Chem. Phys. Chem.* **2004**, *5*, 1106–1120.

- (22) Gan, Q.; Rooney, D.; Xue, M.; Thompson, G.; Zou, Y. An experimental study of gas transport and separation properties of ionic liquids supported on nano filtration membranes. *J. Membr. Sci.* **2006**, *280*, 948–956.

- (23) Fredlake, C. P.; Crosthwaite, J. M.; Hert, D. G.; Aki, S. N. V. K.; Brennecke, J. F. Thermophysical properties of imidazolium-based ionic liquids. *J. Chem. Eng. Data* **2004**, *49*, 954–964.

- (24) Zhang, S.; Sun, N.; He, X.; Lu, X.; Zhang, X. Physical properties of ionic liquids: database and evaluation. *J. Phys. Chem. Ref. Data* **2006**, *35*, 1475–1517.

- (25) <http://ilthermo.boulder.nist.gov/ILThermo/mainmenu.uix>.

- (26) Azevedo, R. G.; Esperança, J. M. S. S.; Najdanovic-Visak, V.; Visak, Z. P.; Guedes, H. J. R.; Nunes da Ponte, M.; Rebelo, L. P. N. Thermophysical and thermodynamic properties of 1-butyl-3-methylimidazolium tetrafluoroborate and 1-butyl-3-methylimidazoliumhexafluorophosphate over an extended pressure range. *J. Chem. Eng. Data* **2005**, *50*, 997–1088.

- (27) Azevedo, R. G.; Esperança, J. M. S. S.; Szydłowski, J.; Visak, Z. P.; Pires, P. F.; Guedes, H. J. R.; Rebelo, L. P. N. Thermophysical and thermodynamic properties of ionic liquids over an extended pressure range: [bmim][NTf<sub>2</sub>] and [hmim][NTf<sub>2</sub>]. *J. Chem. Thermodyn.* **2005**, *37*, 888–899.

- (28) Esperança, J. M. S. S.; Guedes, H. J. R.; Blesic, M.; Rebelo, L. P. N. Densities and derived thermodynamic properties of ionic liquids. 3. Phosphonium-based ionic liquids over an extended pressure range. *J. Chem. Eng. Data* **2006**, *51*, 237–242.
- (29) Esperança, J. M. S. S.; Visak, Z. P.; Pletchkova, N. V.; Seddon, K. R.; Guedes, H. J. R.; Rebelo, L. P. N. Densities and derived thermodynamic properties of ionic liquids. 3. [C3mim][NTf<sub>2</sub>] and [C5mim][NTf<sub>2</sub>]. *J. Chem. Eng. Data* **2006**, *51*, 2009–2015.
- (30) Pereira, A. B.; Verdia, P.; Tojo, E.; Rodriguez, A. Physical properties of 1-butyl-3-methylimidazolium methyl sulfate as a function of temperature. *J. Chem. Eng. Data* **2007**, *52*, 377–380.
- (31) Gardas, R. L.; Freire, M. G.; Carvalho, P. J.; Marrucho, I. M.; Fonseca, I. M. A.; Ferreira, A. G. M.; Coutinho, J. A. P. High-pressure densities and derived thermodynamic properties of imidazolium-based ionic liquids. *J. Chem. Eng. Data* **2007**, *52*, 80–88.
- (32) Gardas, R. L.; Freire, M. G.; Carvalho, P. J.; Marrucho, I. M.; Fonseca, I. M. A.; Ferreira, A. G. M.; Coutinho, J. A. P. P $\rho$ T measurements of imidazolium-based ionic liquids. *J. Chem. Eng. Data* **2007**, *52*, 1881–1888.
- (33) Tomé, L. I. N.; Carvalho, P. J.; Freire, M. G.; Marrucho, I. M.; Fonseca, I. M. A.; Ferreira, A. G. M.; Coutinho, J. A. P.; Gardas, R. L. Measurements and correlation of high-pressure densities of imidazolium-based ionic liquids. *J. Chem. Eng. Data* **2008**, *53*, 1914–1921.
- (34) Gardas, R. L.; Costa, H. F.; Freire, M. G.; Carvalho, P. J.; Marrucho, I. M.; Fonseca, I. M. A.; Ferreira, A. G. M.; Coutinho, J. A. P. Densities and derived thermodynamic properties of imidazolium-, pyridinium-, pyrrolidinium- and piperidinium-based ionic liquids. *J. Chem. Eng. Data* **2008**, *53*, 805–811.
- (35) Gu, Z.; Brennecke, J. F. Volume expansivities and isothermal compressibilities of imidazolium and pyridinium-based ionic liquids. *J. Chem. Eng. Data* **2002**, *47*, 339–345.
- (36) Harris, K. R.; Woolf, L. A.; Kanakubo, M. Temperature and pressure dependence of the viscosity of the ionic liquid 1-butyl-3-methylimidazolium hexafluorophosphate. *J. Chem. Eng. Data* **2005**, *50*, 1777–1782.
- (37) Harris, K. R.; Kanakubo, M.; Woolf, L. A. Temperature and pressure dependence of the viscosity of the ionic liquids 1-methyl-3-octylimidazolium hexafluorophosphate and 1-methyl-3-octylimidazolium tetrafluoroborate. *J. Chem. Eng. Data* **2006**, *51*, 1161–1167.
- (38) Paulechka, Y. U.; Kabo, G. J.; Blokhin, A. V.; Shaplov, A. S.; Lozinskaya, E. I.; Vygodskii, Y. S. Thermodynamic properties of 1-alkyl-3-methylimidazolium bromide ionic liquids. *J. Chem. Thermodyn.* **2007**, *39*, 158–166.
- (39) Papaiconomou, N.; Salminen, J.; Lee, J.-M.; Prausnitz, J. M. Physicochemical properties of hydrophobic ionic liquids containing 1-octylpyridinium, 1-octyl-2-methylpyridinium or 1-octyl-4-methylpyridinium cations. *J. Chem. Eng. Data* **2007**, *52*, 833–840.
- (40) Castro, C. A. N.; Langa, E.; Morais, A. L.; Lopes, M. L. M.; Lourenço, M. J. V.; Santos, F. J. V.; Santos, M. S. C. S.; Canongia Lopes, J. N.; Veiga, H. I. M.; Macatrão, M.; Esperança, J. M. S. S.; Marques, C. S.; Rebelo, L. P. N.; Afeonso, C. A. M. Studies on the density, heat capacity, surface tension and infinite dilution diffusion with the ionic liquids [C4mim][NTf<sub>2</sub>], [C4mim][dca], [C2mim][EtOSO<sub>3</sub>] and [Aliquat][dca]. *Fluid Phase Equilib.* **2010**, *294*, 157–179.
- (41) Sesto, R. E. D.; Corley, C.; Robertson, A. J.; Wilkes, J. S. Tetraalkylphosphonium-based ionic liquids. *J. Org. Chem.* **2005**, *69*, 2536–2542.
- (42) Bradaric, C. J.; Downard, A.; Kennedy, C.; Robertson, A. J.; Zhou, Y. H. Industrial preparation of phosphonium ionic liquids. *Green Chem.* **2003**, *5*, 143–152.
- (43) Atefi, F.; Garcia, M. T.; Singer, R. D.; Scammels, P. J. Phosphonium ionic liquids: design, synthesis and evaluation of biodegradability. *Green Chem.* **2009**, *11*, 1595–1604.
- (44) Marták, J.; Schlosser, S. Extraction of lactic acid by phosphonium ionic liquids. *Sep. Purif. Technol.* **2007**, *57*, 483–494.
- (45) Carvalho, P. J.; Regueira, T.; Santos, L. M. N. B. F.; Fernandez, J.; Coutinho, J. A. P. Effect of water on the viscosities and densities of 1-butyl-3-methylimidazolium dicyanamide and 1-butyl-3-methylimidazolium tricyanomethane at atmospheric pressure. *J. Chem. Eng. Data* **2010**, *55*, 645–652.
- (46) Carvalho, P. J.; Álvarez, V. H.; Marrucho, I. M.; Aznar, M.; Coutinho, J. A. P. High carbon dioxide solubilities in trihexyltetradecylphosphonium-based ionic liquids. *Supercrit. Fluids* **2010**, *52*, 258–265.
- (47) Carvalho, P. J.; Coutinho, J. A. P. On the nonideality of CO<sub>2</sub> solutions in ionic liquids and other low volatile solvents. *J. Phys. Chem. Lett.* **2010**, *1*, 774–780.
- (48) Ventura, S. P. M.; Pauly, J.; Daridon, J. L.; Lopes da Silva, J. A.; Marrucho, I. M.; Dias, A. M. A.; Coutinho, J. A. P. High pressure solubility data of carbon dioxide in tri-iso-butyl(methyl)phosphonium tosylate-water systems. *J. Chem. Thermodyn.* **2008**, *40*, 1187–1192.
- (49) Cornmell, R. J.; Winder, C. L.; Schuler, S.; Goodacre, R.; Stephens, G. Using a biphasic ionic liquid/water reaction system to improve oxygenase-catalysed biotransformation with whole cells. *Green Chem.* **2008**, *10*, 685–691.
- (50) Neves, C. M. S. S.; Freire, M. G.; Robertson, A. J.; Coutinho, J. A. P. Separation of ethanol-water mixtures using phosphonium ionic liquids. 2010, submitted for publication.
- (51) Liu, Y.; Guo, L.; Zhu, L.; Sun, X.; Chen, J. Removal of Cr(III, VI) by quaternary ammonium and quaternary phosphonium ionic liquids functionalized silica materials. *Chem. Eng. J.* **2010**, *158*, 108–114.
- (52) Mokhodoeva, O. B.; Myasoedova, G. V.; Kubrakova, I. V.; Nikulin, O. I.; Artyushin, O. I.; Odinet, I. L. New solid extractants for preconcentrating noble metals. *J. Anal. Chem.* **2010**, *65*, 12–16.
- (53) Stojanovic, A.; Kogelnig, D.; Fischer, L.; Hann, S.; Galanski, M.; Groessl, M.; Krachler, R.; Keppler, B. K. Phosphonium and ammonium ionic liquids with aromatic anions: synthesis, properties and platinum extraction. *Aust. J. Chem.* **2010**, *63*, 511–524.
- (54) Oliveira, F. S.; Freire, M. G.; Pratas, M. J.; Pauly, J.; Daridon, J. L.; Marrucho, I. M.; Coutinho, J. A. P. Solubility of adamantane in phosphonium-based ionic liquids. *J. Chem. Eng. Data* **2010**, *55*, 662–665.
- (55) Kilaru, P. K.; Scovazzo, S. Correlations of low-pressure carbon dioxide and hydrocarbon solubilities in imidazolium-, phosphonium- and ammonium-based room temperature ionic liquids. Part 2. Using activation energy of viscosity. *Ind. Eng. Chem. Res.* **2008**, *47*, 910–919.
- (56) Dymond, J. H.; Malhotra, R. The Tait equation: 100 years on. *Int. J. Thermophys.* **1988**, *9*, 941–951.
- (57) Sanchez, I. C.; Lacombe, R. H. Statistical thermodynamics of polymer solutions. *Macromolecules* **1978**, *11*, 1145–1156.
- (58) Dee, G. T.; Walsh, D. J. Equation of state for polymer liquids. *Macromolecules* **1988**, *21*, 811–815.
- (59) Dee, G. T.; Walsh, D. J. A modified cell model equation of state for polymer liquids. *Macromolecules* **1988**, 815–817.
- (60) Gardas, R. L.; Coutinho, J. A. P. Extension of the Ye and Shreeve group contribution method for density estimation of ionic liquids in a wide range of temperatures and pressures. *Fluid Phase Equilib.* **2008**, *263*, 26–32.
- (61) Kilaru, P. K.; Baker, G. A.; Scovazzo, P. Density and Surface Tension Measurements of Imidazolium-, Quaternary Phosphonium-, and Ammonium-Based Room-Temperature Ionic Liquids: Data and Correlations. *J. Chem. Eng. Data* **2007**, *52*, 2306–2314.
- (62) Neves, C. M. S. S.; Carvalho, P. J.; Freire, M. G.; Coutinho, J. A. P. Thermophysical Properties of Neat and Water Saturated Tetradecyltrihexylphosphonium-based Ionic Liquids. *J. Chem. Thermodyn.* **2010**, DOI: 10.1016/j.jct.2011.01.016.
- (63) Piñeiro, M. M.; Bessières, D.; Saint-Guirons, H.; Legido, J. L. Measurements of Nonfluorobutyl Methyl Ether and Nonfluorobutyl Ethyl Ether between 283.15 and 323.15 K at Pressures up to 40 MPa. *Int. J. Thermophys.* **2003**, *24*, 1265–1276.
- (64) Piñeiro, M. M.; Bessières, D.; Gacio, J. M.; Saint-Guirons, H.; Legido, J. L. Determination of high-pressure liquid density for n-perfluorohexane and n-perfluorononane. *Fluid Phase Equilib.* **2004**, *220*, 127–136.
- (65) Huddleston, J. G.; Visser, A. E. R.; Willauer, H. D.; Broker, G. A.; Rogers, R. D. Characterization and comparison of hydrophilic and hydrophobic room temperature ionic liquids incorporating the imidazolium cation. *Green Chem.* **2001**, *3*, 156–164.

(66) Machida, H.; Sato, Y.; Smith, R. L. J. Pressure-volume-temperature (PVT) measurements of ionic liquids ([bmim+][PF6-], [bmim+][BF4-], [bmim+][OcSO4-]) and analysis with the Sanchez-Lacombe equation of state. *Fluid Phase Equilib.* **2008**, *264*, 147–155.

(67) Sato, Y.; Hashiguchi, H.; Takishima, S.; Masuoka, H. Prediction of PVT properties of polymer melts with a new group-contribution equation of state. *Fluid Phase Equilib.* **1998**, *144*, 427–440.

(68) Ye, C.; Shreeve, J. M. Rapid and accurate estimation of densities of room-temperature ionic liquids and salts. *J. Phys. Chem. A* **2007**, *111*, 1456–1461.

(69) Machida, H.; Taguchi, R.; Sato, Y.; Smith, R. L. J. Analysis of ionic liquid PVT behavior with a Modified Cell Model. *Fluid Phase Equilib.* **2009**, *281*, 127–132.